PCCP

PAPER

View Article Online
View Journal | View Issue

Cite this: *Phys. Chem. Chem. Phys.*, 2018, **20**, 11437

Stability of the zwitterionic liquid butyl-methyl-imidazol-2-ylidene borane†

Steffen Tröger-Müller, Markus Antonietti and Clemens Liedel *

Received 15th January 2018,
Accepted 26th March 2018

DOI: 10.1039/c8cp00311d

rsc.li/pccp

Modification of the C2 position of the standard 1-butyl-3-methyl imidazolium cation by a borohydride group leads to a zwitterionic liquid (**ZIL**). The resulting imidazol-2-ylidene borane **ZIL** is liquid at room temperature. Dynamic viscosity as well as thermal and electrochemical stability are investigated. Thermal decomposition follows a similar pathway as in comparable imidazolium ionic liquids. The surprisingly low viscosity and good reductive stability make it a promising candidate for electrochemical applications.

Introduction

Imidazolium ionic liquids (ImILs) are a well understood and versatile class of ionic liquids. As most ILs they are usually of low-flammability, have negligible vapor pressure, and can be easily tuned to their prospective applications by proper design and choice of anion and cation.[1] As an additional benefit, they may be obtained without the use of alkylation reactions[2] and from biomass,[3] which improves their ecological footprint and allows for truly green chemistry. They are applied in various fields ranging from industrial chemistry[1] and catalysis[4] over biomass treatment[5,6] to electrochemistry and energy storage R&D.[7] In all those applications, viscosity and stability play a prominent role. Both may be optimized by proper choice of cation and anion and are often based on the special reactivity of the imidazolium ring.

Thermal stability is usually limited by cleavage of the N–C bonds of the alkyl chains pendant on the imidazolium ring (thermally induced or by nucleophilic attack of the counterion with increased reactivity at elevated temperatures).[8] Attempts to increase the thermal stability of imidazolium ionic liquids consequently include the introduction of non-nucleophilic counterions.

The carbon atom at the 2-position (C2, between both nitrogen atoms) is the most electron deficient atom of the aromatic heterocycle and the main reason for concerns about its chemical stability.[9,10] Its electron deficiency makes it prone to nucleophilic attack which may lead to degradation by ring opening.[11] It also weakens the bond to its pendant proton, causing it to be rather acidic (with typical pK_a values around 20–22).[12] Abstraction of the proton eventually leads to the formation of N-heterocyclic carbenes (NHC) which are highly reactive species themselves[11] even though their stability is higher when compared to other carbenes.[13]

Limited electrochemical stability bears on the electron deficiency at the C2 carbon where reduction preferentially occurs. This is also the most probable location of the unpaired electron in the resulting neutral radical,[10] which may then undergo further reaction, *e.g.*, with itself to form dimers, disproportionate, or devolve into a carbene.[9]

In order to increase the (electro-)chemical stability of ImILs, protection of the C2 position with alkyl groups, most notably simple methyl groups, is a viable approach. Resulting C2-methylated ImILs are more stable against Grignard reagents[14] or against chemical[15] and electrochemical reduction.[10] Unfortunately, protection with methyl groups has been shown to increase the viscosity,[16,17] which is a big trade-off in the context of possible applications and general manageability of the resulting compounds. The unusually large increase of viscosity may be attributed to a suppression of the mobility of the counterion. Its ability to move around the imidazolium ring *via* favorable interaction with the C2 position is impeded upon C2 substitution.[17] To decrease viscosity and lower the glass transition temperature, bulky, less interacting counterions like bis(trifluoromethanesulfonyl)imide (TFSI) are commonly introduced. In contrast, Gardner *et al.* have recently published a facile route to substitute the hydrogen at the C2 position with a BH_3-group.[18,19] The resulting imidazol-2-ylidene borane compounds, so far as they are liquid, show comparatively low viscosities.[20]

NHC-boranes combine good stability with reducing ability and have even been shown to participate in metal complexes.[21] This makes them interesting candidates for electrochemical

Department of Colloid Chemistry, Max Planck Institute of Colloids and Interfaces Research Campus Golm, 14476 Potsdam, Germany.
E-mail: Clemens.Liedel@mpikg.mpg.de

† Electronic supplementary information (ESI) available: NMR spectra, DSC, shear stress–shear rate curves, TGA–MS curves. See DOI: 10.1039/c8cp00311d

applications. Excited by the simple route to access those unique compounds, we set out to evaluate the stability of one such imidazol-2-ylidene borane zwitterionic liquid (**ZIL**). We investigate thermal and electrochemical decomposition and compare it to similar imidazolium ionic liquids with TFSI counterion or methylated C2 position.

Results and discussion

We synthesized 1-butyl-3-methylimidazol-2-ylidene borane (**ZIL**) from 1-butyl-3-methylimidazolium iodide (**IL-H-I**) by reaction with sodium borohydride at elevated temperature. Structurally similar imidazolium ionic liquids with different anions and unprotected (**IL-H-I** and 1-butyl-3-methylimidazolium bis(trifluoromethanesulfonyl)imide (**IL-H-TFSI**)) or protected C2 position (1-butyl-2,3-dimethylimidazolium iodide (**IL-Me-I**) and 1-butyl-2,3-dimethylimidazolium bis(trifluoromethanesulfonyl)imide (**IL-Me-TFSI**)) were synthesized according to the literature for comparison.[19,20] In the abbreviations of ILs, the middle part denotes the group at C2 while the last part indicates the counterion. All compounds were dried in vacuum. Chart 1 displays the different ionic liquids.

Even though C2 modification of ImILs is known to increase the glass transition temperature T_G,[14,22] the **ZIL** stays liquid even after prolonged drying in vacuum. Differential scanning calorimetry (DSC) measurements in Fig. 1 demonstrate that T_G is as low as −64.9 °C, similar to T_G of **IL-H-I** (−68.3 °C). The anticipated and observed increase of T_G upon C2 methylation (**IL-Me-I**, which is solid at room temperature, *vs.* **IL-H-I** or **IL-Me-TFSI** *vs.* **IL-H-TFSI**) hence does not occur when the C2 position in imidazolium is protected by a BH_3 group instead of a methyl group. As expected, ionic liquids with TFSI anion have a lower T_G (and in the case of **IL-H-TFSI** exhibit cold crystallization).[23] Substitution of the C2 position with a methyl group in **IL-Me-TFSI** seems to suppress the cold crystallization.

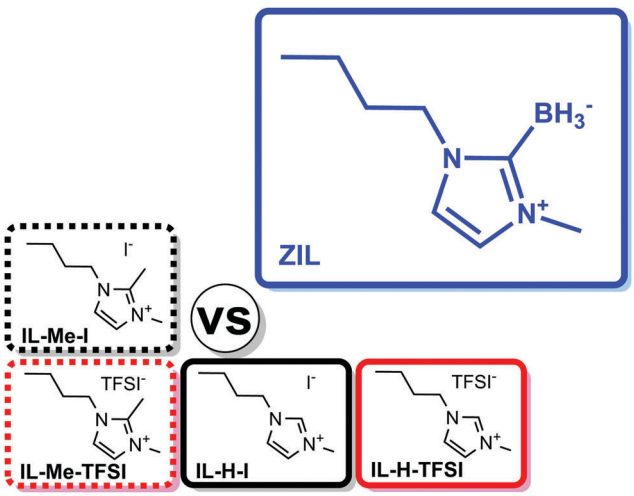

Chart 1 Overview of the relevant ionic systems compared in this work. Colors are used in figures throughout this work to refer to the corresponding compounds.

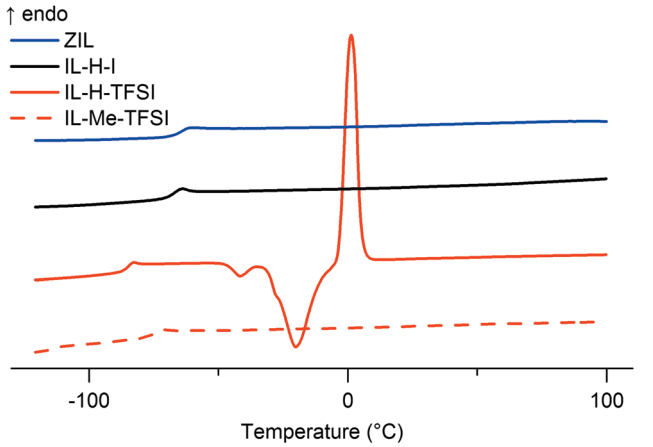

Fig. 1 Differential scanning calorimetry of the **ZIL** as well as **IL-H-I**, **IL-H-TFSI**, and **IL-Me-TFSI** (**IL-Me-I** is a solid). The figure shows the temperature region between −120 °C and 100 °C, revealing glass transitions in all displayed graphs (**ZIL**: −64.9 °C; **IL-H-I**: −68.3 °C; **IL-H-TFSI**: −85.5 °C; **IL-Me-TFSI**: −75.4 °C) as well as cold crystallization (−41.5 °C, −20.1 °C) and consecutive melting (1.3 °C) in the case of **IL-H-TFSI** (individual graphs and further details see ESI†).

Since the notion of a liquid zwitterionic compound is somewhat counterintuitive, we will discuss this in more detail. Lewis acid/Lewis base pairs based on N-heterocyclic carbenes and boron compounds have been described in the literature, including discussions on stability, X-ray structures, and spectroscopy.[21] These so called NHC-boranes find applications as co-initiators in radical polymerization, reagents, or catalysts. Interestingly, the structures are quite stable, and the borane compounds do not usually hydroborate themselves.[21] Concerning the charge, in the resonance structure of 1,3-bis(2,6-diisopropylphenyl)imidazol-2-ylidene borane, the positive charge is not only located at the nitrogen but also partly at the C2 position, and the orbital model resembles an N-heterocyclic carbene with a C–B bond formed from the electron rich C2 σ orbital. As for NHC-boranes of lesser steric demand, Huang *et al.* have used electrostatic potential analysis to show that the Hirshfield charge on 1,3-dimethylimidazol-2-ylidene borane (which is very similar to the **ZIL** described here) is (i) indeed separated and (ii) the positive charge (0.456 *e*) is delocalized over the imidazolium ring, while the negative charge (−0.456 *e*) is carried by the BH_3-group.[20] Furthermore, X-ray crystallographic analysis has confirmed the structure of said NHC-borane and revealed a C2–B bond length of 1.596 Å in the same study. Since the **ZIL** is liquid up to very low temperatures, crystallographic analysis is not readily available (investigations using combined X-ray diffraction studies with zone melting as described by Choudhury *et al.*[24] would in our case require infeasible setups with temperatures in the range of −100 °C inside the spectrometer), but the presence of a C2–B bond can be deduced from ^{13}C nuclear magnetic resonance (NMR) spectra. Fig. 2 shows the proton decoupled ^{13}C NMR spectra of the **ZIL** and **IL-H-I**. The spectra show the same peaks with minor differences in chemical shift with one exception. The signal of the C2 carbon is shifted downfield in the **ZIL**, the intensity is drastically reduced, and it

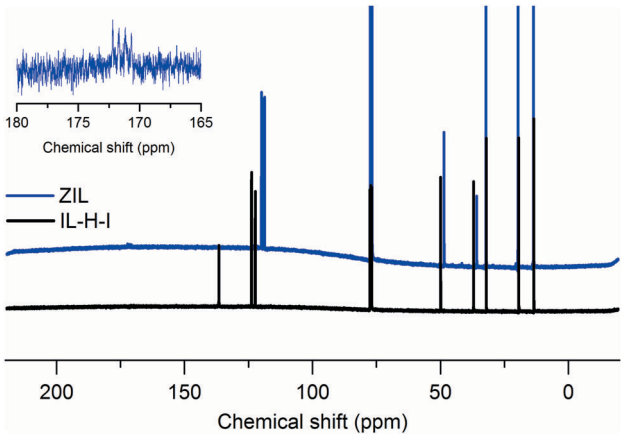

Fig. 2 ^{13}C nuclear magnetic resonance spectra of the **ZIL** and **IL-H-I**. The inset shows the signal of the C2 carbon of the **ZIL**.

is split into a quartet with approximately 1 : 1 : 1 : 1 intensities, just as expected for C–B bonds in proton decoupled ^{13}C NMR spectra.[25] Drawing upon these results, the **ZIL** qualifies as a room temperature zwitterionic liquid. **IL-H-I**, **IL-H-TFSI**, and **IL-Me-TFSI** are room temperature ionic liquids. We note that the synthesized **ZIL** is a reducing agent,[18] and the presence of reducing agents interferes with Karl–Fischer titration.[26] Hence we could not quantitatively determine the water content, which may also contribute to liquidity of ILs.[27] Instead, water content was estimated by thermogravimetric analysis (TGA) to be within the range of expectation for ionic liquids. While upon heating the extensively vacuum dried species to 120 °C in the TGA the **ZIL** loses 1.93% of its weight, within this temperature range several decomposition products appear (see below and ESI†), so the weight loss only partly may denote to water, and the water content is significantly lower than that.

The performance of ionic liquids depends on their viscosity in all fields that rely on mass transport properties, where low viscosity is usually favorable. On a general level a multitude of factors, such as temperature, nature of the anion, cationic structure, or additives, may influence the viscosity of ionic liquids.[6,28] As noted above, substitutions at the C2 position may effect a specially strong increase in viscosity. To investigate the influence of the BH_3 group, we evaluated the dynamic viscosity at room temperature using shear stress–shear rate curves of the dried samples (see ESI†). Table 1 lists the obtained viscosities in comparison to the viscosity of water.

Table 1 Dynamic viscosities of the **ZIL** and the ILs. The viscosity of water is added for comparison. All viscosities were measured at 25 °C

Sample	Viscosity (cP)	Error	Water content[a] (wt%)
ZIL	181	±0.46	[b]
IL-H-I	668	±4	2.43
IL-Me-I	Solid at RT	—	0.89
IL-H-TFSI	48	±0.012	0.01
IL-Me-TFSI	108	±0.173	0.13
Water[29]	0.89	None given	

[a] Water content was determined from TGA mass loss at 120 °C. [b] See text.

As expected, comparison of **IL-H-I** and **IL-H-TFSI** to their C2 methylated counterparts **IL-Me-I** and **IL-Me-TFSI** reveals a drastic increase in viscosity (viscosity increases by 125% in the TFSI based ILs, and **IL-Me-I** is even a solid). This agrees with the model explored by Izgorodina *et al.*[17] whereby C2 substitution decreases the mobility of the counterion in 1-methyl-3-propyl-imidazolium iodide.

Hydroboration of the C2 position does not follow this trend. The viscosity of the **ZIL** is drastically lower than that of **IL-H-I** and **IL-Me-I**. It follows a similar trend as exchange of the iodine in **IL-H-I** and **IL-Me-I** by TFSI in **IL-H-TFSI** and **IL-Me-TFSI**, respectively, which also leads to drastically reduced viscosity. While in the latter case decreased interaction between anion and cation and hence higher mobility is probably responsible for decreased viscosity, this explanation would intuitively result in the opposite behavior, *i.e.*, increasing viscosity, when comparing the **ZIL** to **IL-H-I** or **IL-Me-I**.

Hence, a different physical mechanism must be responsible for the decreased viscosity in the **ZIL**: in comparison to **IL-H-I** and **IL-Me-I**, where the anion is preferentially located above or below the plane of the imidazolium ring,[17] the anion is fixed perpendicular to the ring in the **ZIL**. The 2-dimensionality of the structure creates a fundamentally different situation compared to traditional ionic liquids where anion–cation interactions play a bigger role. Instead of an ionic species, the **ZIL** may also be described as polar molecule with a lower molecular weight (152.15 g mol^{-1}) than the ionics **IL-H-I** (266.03 g mol^{-1}), **IL-Me-I** (280.04 g mol^{-1}), **IL-H-TFSI** (419.04 g mol^{-1}), and **IL-Me-TFSI** (433.06 g mol^{-1}). Low molecular weight often also implies high mobility[30] and may contribute to the comparably low viscosity observed for the **ZIL**. We note that low viscosity of the **ZIL** may not be attributed to high water content since it is much lower than in **IL-H-I** (with the exact amount unfortunately unknown as described above) while viscosity is also significantly lower. We also note that the viscosity of all samples was recorded using the dried samples and decreases upon exposure to air and uptake of water from the atmosphere (see ESI†). Summarizing this part, hydroboration of the C2 position of an imidazolium IL leads to low viscosity without the introduction of bulky anions.

In order to evaluate the stability of the **ZIL** in comparison to the standard ionic liquids **IL-H-I** and **IL-H-TFSI** as well as their C2 methylated counterparts **IL-Me-I** and **IL-Me-TFSI**, thermal and electrochemical decomposition were evaluated by thermogravimetric analysis (TGA) and linear sweep voltammetry (LSV), respectively. Fig. 3 displays the results of TGA measurements. While methylation of the C2 position has only a little effect on the thermal stability, hydroboration of the C2 position clearly leads to decreased thermal stability (onset of decomposition at 202 °C, compared to 284 °C for **IL-H-I** and 425 °C for **IL-H-TFSI**). High thermal stability of **IL-H-TFSI** may be attributed to the almost negligible nucleophilicity of the bulky TFSI anion compared to the far more nucleophilic iodide in **IL-H-I**.

In order to understand the reason for the decreased stability, we investigated decomposition products of the **ZIL** during heating in more detail. We especially focused on three possible decomposition

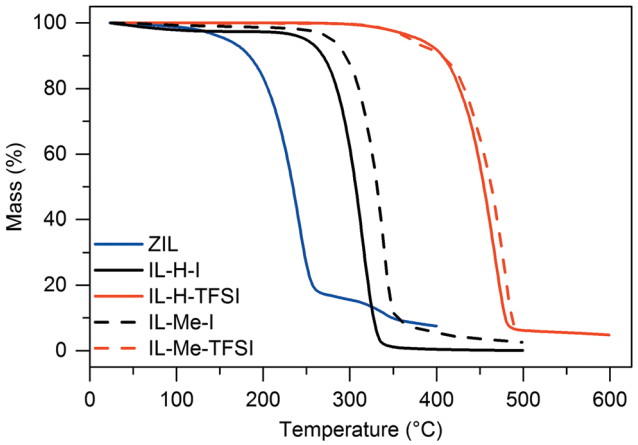

Fig. 3 Thermogravimetric analysis of the **ZIL** and the ILs. Data was acquired at a scan rate of 10 K min^{-1}.

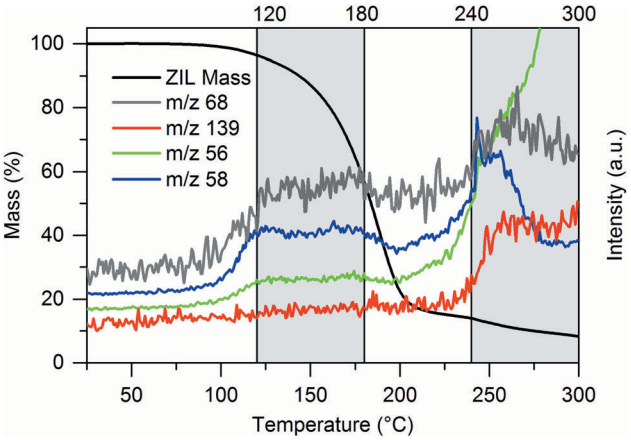

Fig. 5 Decomposition of the **ZIL**: some representative examples of TGA–MS analysis recorded at a heating rate of 2.5 K min^{-1}. From the data we obtain two general regions of decomposition. More ion currents are summarized in the ESI.† Left axis of ordinates corresponds to mass loss (black line), right axis of ordinates to the other curves.

pathways as outlined in Fig. 4. In short, we anticipated (1) dissociation of the carbon–boron bond; (2) the decomposition by ring opening after attack at the C2 position; (3) the cleavage of carbon–nitrogen bonds. With regard to the pathways 2 and 3 we assumed that the borohydride group of the **ZIL** shows similar behavior as borohydride salts and acts as donor of formally nucleophilic hydrogen.

We evaluated the proposed decomposition pathways of the **ZIL** by TGA coupled with mass spectroscopy (TGA–MS). The mass profile of the TGA–MS curve and ion current graphs that show representative shapes are displayed in Fig. 5. Further ion currents indicating other decomposition products are shown in the ESI.† We note that TGA–MS was performed at significantly decreased heating rate of 2.5 K min^{-1} (compared to 10 K min^{-1} in Fig. 3), resulting in different apparent thermal stability.

Fig. 5 shows two plateaus/peaks in the ion current curves which correspond to two steps of mass loss from TGA–MS measurement, which may indicate two distinct decomposition steps. In the first step, decomposition products from pathway 3-a (cleavage of the carbon–nitrogen bond at the butyl side chain) prominently appear, together with H_2 as the main decomposition product. In the second step, decomposition products from pathways 3-a (cleavage of the carbon–nitrogen bond at the methyl side chain) and 1 (cleavage of the carbon–boron bond) appear. TGA–MS data could not confirm decomposition by ring opening (pathway 2). In contrast, occurrence of imidazole (*m*/*z* 68) already in the first decomposition step indicates that cleavage of the C–B bond (pathway 1) also happens already at this temperature. The two step detection of mass loss may thus also be explained by different volatility. Recombination of decomposition products also happens, since dimethyl-2-*H*-imidazole was also detected, as was the original cation 1-butyl-3-methylimidazolium.

Pathway 3 is also the main thermal decomposition mechanism for normal (not zwitterionic) imidazolium ionic liquids.[8] In the **ZIL**, the BH_3 group acts as reducing agent and initiates nucleophilic attack,[18] leaving saturated butane and methane as well as dealkylated imidazol-2-ylidene boranes as decomposition products. The lower overall thermal stability implies that the nucleophilic attack by BH_3 actually is favored compared to conventional counterions.

Two things should be noted on TGA–MS data. (i) From the *m*/*z* values it is not possible to distinguish the imidazoles (see Fig. 4, decomposition products 1-c) from their isomeric carbenes. We assume the detected species to be the imidazoles because they are thermodynamically more stable than the carbenes. (ii) The dissociation of the carbon–boron bond does not seem to result in the formation of the 1,3-dialkylated carbene (1-a), or the carbene reacts faster than it can be detected. Moreover, removal of the BH_3 group seems to result in formation of the ionic liquid cation (1-b).

Besides thermal stability, we also assessed the electrochemical stability of the **ZIL** by linear sweep voltammetry on 316 stainless steel working electrodes *vs.* lithium counter electrodes and compared it to **IL-H-I**, **IL-H-TFSI**, and **IL-Me-TFSI**. The results are shown in Fig. 6. In this experiment, we define stability for a current flow only below 0.15 mA (dashed lines in Fig. 6). With this limit, we found the **ZIL** to be quite stable with a reductive stability of −0.14 V *vs.* Li^+/Li and an oxidative stability of 3.72 V *vs.* Li^+/Li. The resulting electrochemical window is 3.86 V.

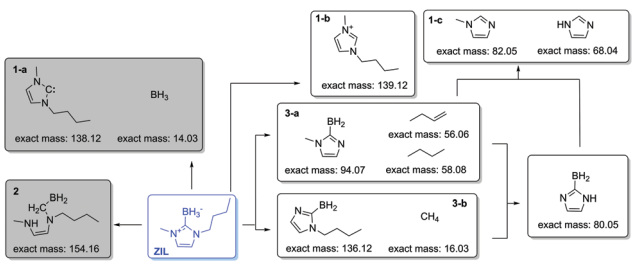

Fig. 4 The main decomposition pathways of the **ZIL** investigated by TGA–MS and masses of main fragments: (1) dissociation of the carbon–boron bond. (2) Decomposition by ring opening. (3) Cleavage of the carbon–nitrogen bond. Grey boxes show assumed decomposition mechanisms that could not be verified.

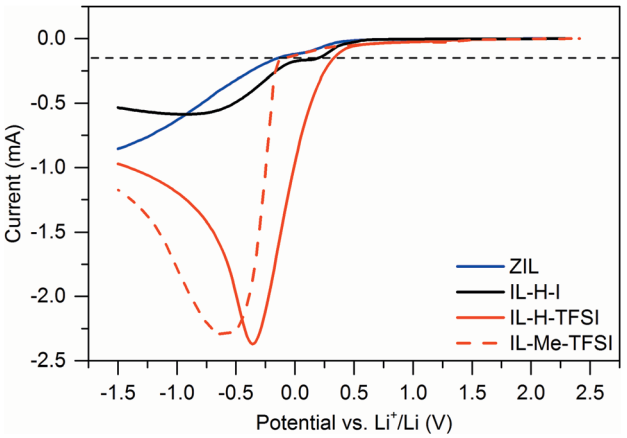

Fig. 6 Linear sweep voltammograms of the **ZIL**, **IL-H-I**, **IL-H-TFSI**, and **IL-Me-TFSI**. Curves were recorded at 5 mV s^{-1} on 316 stainless steel electrodes.

Concerning reductive stability, it is known to be enhanced upon protection of the C2 position in ImILs by methyl groups[10] (here: −0.08 V *vs.* Li^+/Li in the case of **IL-Me-TFSI** compared to 0.33 V *vs.* Li^+/Li for **IL-H-TFSI**), as shown also in Fig. 6. Protection by borohydride groups results in roughly the same (even slightly better) enhancement in reductive stability. Stability in both cases (**ZIL** and **IL-Me-TFSI**) is significantly better than in the unprotected comparable ILs **IL-H-I** (0.20 V *vs.* Li^+/Li) and **IL-H-TFSI**, indicating that C2 protection with a borohydride group has a similar effect on stability as using ILs with methylated C2 positions. The shape of the LSV curve also reveals that the electrochemical decomposition behavior of the **ZIL** is similar to decomposition of the iodide containing **IL-H-I** and differs from the TFSI containing **IL-H-TFSI** and **IL-Me-TFSI**, where TFSI decomposition may appear.

Oxidative stability of the **ZIL** is higher than the stability limit of **IL-H-I**. In the latter, decomposition is attributed to the onset of iodide oxidation (here: 3.19 V *vs.* Li^+/Li). Still, as expected the **ZIL** is a reducing agent, and the stabilities of both TFSI based ionic liquids are higher (5.66 V and 5.48 V *vs.* Li^+/Li for **IL-Me-TFSI** and **IL-H-TFSI**, respectively). Finally, it is noteworthy that water content of the **ZIL** or the ILs does not seem to negatively influence the electrochemical behavior (current flow below 0.15 mA may result from water reduction).

Experimental

Materials

1-Methylimidazol (≥99%, purified by redistillation) and dichloromethane (99.9% by GC) were obtained from Sigma-Aldrich, 1-iodobutane (99%) and chloroform-d (99.8%D) were obtained from Aldrich, toluene (99.7% by GC) was obtained from Honeywell, sodium borohydride (99%) was obtained from Acros, and lithium bis(trifluoromethanesulfonyl)imide (99%) was obtained from Io-Li-Tec.

Methods

Thermogravimetric analysis (TGA). Thermogravimetric analysis (TGA) measurements were performed using a thermo microbalance TG 209 F1 Libra (Netzsch, Selb, Germany). An aluminum crucible was used for the measurement in a nitrogen flow of 20 ml min^{-1} and a purge flow of 20 ml min^{-1} (oxygen flow 10 ml min^{-1}) at a heating rate of 10 K min^{-1}. TGA–MS measurements were performed at a heating rate of 2.5 K min^{-1} using the same microbalance coupled with a Thermostar mass spectrometer (Pfeiffer Vacuum, Asslar, Germany) with an ionization energy of 75 eV.

Differential scanning calorimetry (DSC). Differential scanning calorimetry (DSC) was conducted using a Mettler-Toledo DSC1 STARe system. Glass transition temperatures were determined using the Mettler-Toledo STARe software V9.30. Glass transition temperatures refer to the midpoint of the glass transition; crystallization temperatures refer to the peak temperature. Samples were heated from room temperature to 100 °C and subsequently cooled to −150 °C. The heating and cooling cycle was repeated between 100 °C and −150 °C two times, once to completely remove any thermal history of the sample and once to collect the DSC data. Measurements were conducted at a heating rate of 10 K min^{-1} under nitrogen atmosphere. DSC data displayed in this work shows heating curves.

Viscosity. Viscosity was measured using a stress-controlled rotational rheometer MCR 301 (Anton Paar) equipped with a 12 mm diameter cone–plate geometry with a 1° cone angle and a 20 μm truncation (torque sensor resolution 1 μN m). Viscosity was calculated by linear regression of shear stress–shear rate curves (500 to 3000 s^{-1} at 25 °C) recorded under ambient atmosphere at a humidity of *ca.* 37% immediately after taking the sample out of the glove box as well as after equilibration with ambient air.

Electrochemical testing. The ionic liquids were dried for one day at room temperature and for another day at 60 °C under high vacuum (10^{-3} mbar) prior to use for electrochemistry. Electrochemical cells (two-electrode Swagelok-type cells) were prepared in a Unilab MBraun argon filled glove box (water and oxygen below 0.1 ppm), working electrodes (stainless steel-316) were cleaned with ethanol and acetone prior to polishing them with 1 μm diamonds and 0.05 μm alumina, respectively. After each polishing step electrodes were sonicated for 10 min in 0.06 μS distilled water. Counter electrodes (lithium metal) were scratched with a doctor blade prior to assembly of electrochemical cells to prepare a fresh lithium surface. Electrochemical measurements were conducted using an MPG-2 potentiostat (Bio-Logic). All measurements were conducted at 5 mV s^{-1}.

Nuclear magnetic resonance spectroscopy (NMR) measurements. ^{13}C and ^{1}H NMR measurements were carried out using a Bruker ascend400 Avance III with a Prodigy probe. NMR-spectra were recorded in $CDCl_3$.

Mass spectrometry (MS). A Waters QTof Xevo G2-XS mass spectrometer, connected to a Waters Acquity H-class HPLC for sampling using acetonitrile as the solvent with formic acid as the ionization agent, was used for mass spectrometry of the standard ionic liquids. MS of the ZIL was recorded using a Bruker maXis ESI-Q-TOF using acetonitrile as the solvent and formic acid as the ionization agent.

Synthesis of ionic liquids

1-Butyl-3-methylimidazolium iodide (IL-H-I). Synthesis was adapted from the literature.[19,20] In a typical synthesis, 8 ml 1-methylimidazole (0.100 mol) were dissolved in 30 ml dichloromethane (DCM), and 13.7 ml iodobutane (0.120 mol, 1.2 eq.) were added while the mixture was stirred. The reaction was heated to reflux (50 °C oil bath temperature) and stirred overnight. On the following day the reaction mixture was monitored with NMR-spectroscopy until no imidazole peak was visible and then concentrated *en vacuo*. The so obtained crude product (28.34 g) was used for further reactions without purification (quant. yield). ^{1}H NMR (400 MHz, chloroform-d) δ 9.98 (d, J = 1.7 Hz, 1H), 7.56 (dt, J = 33.5, 1.7 Hz, 4H), 4.32 (t, J = 7.4 Hz, 2H), 4.10 (s, 3H), 1.94–1.84 (m, 3H), 1.41–1.29 (m, 4H), 0.94 (dd, J = 8.2, 6.4 Hz, 5H). (MS, calcd:‡ pos. ion mode ($C_8H_{15}N_2^+$): 139.12 [M^+]; neg. ion mode (I^-): 126.91 [M^-]; MS, found: pos. ion mode ($C_8H_{15}N_2^+$): 139.108 [M^+]; neg. ion mode (I^-): 126.907 [M^-]).

1-Butyl-3-methylimidazol-2-ylidene borane (ZIL). In a typical synthesis 13.32 g (0.05 mol) of **IL-H-I** were dispersed in 50 ml toluene. To the mixture, 2.27 g (0.06 mol, 1.2 eq.) sodium borohydride were added, and the mixture was heated to 105 °C and stirred overnight. On the next day, the hot toluene was decanted into an Erlenmeyer flask and from that flask into a round bottom flask.§ The decantation was repeated twice with fresh toluene, which was always heated to 105 °C prior to decantation. The collected toluene phase was left to settle for one day to allow for precipitation of residual sodium borohydride and then filtered. The toluene was removed by rotary evaporation, and the crude product was dissolved in dichloromethane to allow for further precipitation of sodium borohydride and other solid impurities. After decantation and concentration *en vacuo*, 2.54 g (0.017 mol, 34% yield) of the product were obtained as a clear liquid. 1H NMR (400 MHz, chloroform-d) δ 6.82 (q, J = 2.0 Hz, 2H), 4.14–4.09 (m, 2H), 3.74 (s, 3H), 1.77 (tt, J = 8.8, 6.8 Hz, 2H), 1.36 (dt, J = 14.8, 7.4 Hz, 2H), 0.96 (t, J = 7.4 Hz, 3H). (MS, calcd ($C_8H_{17}BN_2Na^+$, [M + Na^+]): pos. ion mode: 175.1377 [M + Na^+], found 175.1376 [M + Na^+]).

1-Butyl-3-methylimidazolium bis(trifluoromethanesulfonyl)imide (IL-H-TFSI). 14.13 g (0.053 mol) **IL-H-I** were dissolved in 20 ml distilled water, and 18.3 g (0.064 mol, 1.2 eq.) lithium bis(trifluoromethanesulfonyl)imide dissolved in 30 ml distilled water were added. The mixture was stirred overnight at room temperature. The resulting phases were separated, and the hydrophobic phase was washed with water until testing the water phase with silver nitrate did not form a visible precipitate and then one more time after that. The hydrophobic phase was concentrated en vacuo to yield 16.74 g (0.040 mol, 75.5% yield) of the ionic liquid product. ^{1}H NMR (400 MHz, chloroform-d) δ 8.59 (d, J = 2.0 Hz, 1H), 7.31 (dq, J = 7.7, 1.8 Hz, 2H), 4.13–4.08 (m, 2H), 3.87 (d, J = 1.4 Hz, 3H), 1.84–1.74 (m, 2H), 1.36–1.23 (m, 2H), 0.89 (td, J = 7.4, 1.4 Hz, 3H). (MS, calcd: pos. ion mode ($C_8H_{15}N_2^+$): 139.12 [M^+]; neg. ion mode ($C_2F_6NO_4S_2^-$): 279.92 [M^-]; MS, found: pos. ion mode ($C_8H_{15}N_2^+$): 139.118 [M^+]; neg. ion mode ($C_2F_6NO_4S_2^-$): 279.924 [M^-]).

1-Butyl-2,3-dimethylimidazolium iodide (IL-Me-I). 8.87 ml (0.100 mol) of 1,2-dimethylimidazole were dissolved in DCM (30 ml), and 13.7 ml (0.120 mol, 1.2 eq.) iodobutane were added. The mixture was stirred at 60 °C overnight. On the next day the solvent was removed at reduced pressure, and the crude product was dried in vacuum (10^{-3} mbar) at room temperature to reveal a solid product (26.45 g, 0.094 mol, 94% yield) ^{1}H NMR (400 MHz, chloroform-d) δ 7.62 (d, J = 2.1 Hz, 1H), 7.46 (d, J = 2.1 Hz, 1H), 4.20 (t, J = 7.5 Hz, 2H), 4.01 (s, 3H), 2.84 (s, 3H), 1.89–1.80 (m, 2H), 1.43 (dq, J = 14.8, 7.4 Hz, 2H), 0.98 (t, J = 7.3 Hz, 3H). (MS, calcd: pos. ion mode ($C_9H_{17}N_2^+$): 153.14 [M^+]; neg. ion mode (I^-): 126.91 [M^-]; MS, found: pos. ion mode ($C_9H_{17}N_2^+$): 153.138 [M^+]; neg. ion mode (I^-): 126.903 [M^-]).

1-Butyl-2,3-dimethylimidazolium bis(trifluoromethanesulfonyl)-imide (IL-Me-TFSI). 5.35 g (0.019 mol) of **IL-Me-I** were dissolved in 40 ml water. A mixture of 6.86 g (0.024 mol, 1.26 eq.) lithium bis(trifluoromethanesulfonyl)imide in 20 ml water was added, and the mixture was stirred overnight. Two phases formed and were separated on the next day. The (lower) ionic liquid containing layer was washed with water until testing with silver nitrate did not show precipitation anymore. After drying in high vacuum at 60 °C overnight a liquid product was obtained (6.64 g, 0.015 mol, 79% yield). ^{1}H NMR (400 MHz, chloroform-d) δ 7.23 (d, J = 2.1 Hz, 1H), 7.19 (d, J = 2.1 Hz, 1H), 4.07 (t, J = 7.5 Hz, 2H), 3.83 (s, 3H), 2.63 (s, 3H), 1.85–1.75 (m, 2H), 1.40 (dq, J = 14.7, 7.4 Hz, 2H), 0.99 (t, J = 7.4 Hz, 3H). (MS, calcd: pos. ion mode ($C_9H_{17}N_2^+$): 153.14 [M^+]; neg. ion mode ($C_2F_6NO_4S_2^-$): 279.92 [M^-]; MS, found: pos. ion mode ($C_9H_{17}N_2^+$): 153.137 [M^+]; neg. ion mode ($C_2F_6NO_4S_2^-$): 279.917 [M^-]).

Conclusions

With significant enhancement of the electrochemical reductive stability similar to C2-methylation and decrease of the viscosity similar to anion exchange by a bulky anion, zwitterionic liquids with borohydride groups may be an interesting alternative to C2-methylated and TFSI-containing imidazolium ILs. While physical properties are similar, they have several distinct advantages. For example the molecular weight is much lower (152 g mol^{-1} for 1-butyl-3-methylimidazol-2-ylidene borane, *vs.* 433 g mol^{-1} for 1-butyl-2,3-dimethylimidazolium bis(trifluoromethanesulfonyl)imide), making high loading with salts in an electrolyte more likely. The zwitterionic liquid is also far more environmentally benign (not fluorinated), much cheaper, and easy to synthesize. Thermal and oxidative stabilities are lower, owing to the nucleophilicity of the BH_3 group, but sufficient at or around room temperature or moderately increased temperature. Hence, in applications which do not require heating to high temperatures or exposure to strong oxidizers, the presented **ZIL** may be a cheaper

‡ Since ILs consist of ion pairs, M^+ and M^- refer to the molecular ion peaks of cation and anion, respectively. If not denoted otherwise, no additional ionization occurs.

§ This procedure was used so that residual byproduct, which collected in a sticky lower phase, would adhere to the glass wall of the Erlenmeyer flask instead of collecting in the product flask.

and more sustainable alternative to some of the best performing imidazolium ILs.

Conflicts of interest

There are no conflicts to declare.

Acknowledgements

We thank Wuqi Guo for preliminary experiments. We further thank Olaf Niemeyer for fruitful support with NMR measurements, Alberto Sanz de León for rheometer support, Antje Völkel for TGA and TGA–MS, Jessica Brandt and Ursula Lubahn for DSC, as well as Eva Settels and Sylvia Fürstenberg for high resolution MS measurements. Financial support by the Max Planck Society is gratefully acknowledged. Open Access funding provided by the Max Planck Society.

Notes and references

1 N. V. Plechkova and K. R. Seddon, *Chem. Soc. Rev.*, 2008, **37**, 123.
2 D. Depuydt, A. van den Bossche, W. Dehaen and K. Binnemans, *RSC Adv.*, 2016, **6**, 8848; S. Tröger-Müller, J. Brandt, M. Antonietti and C. Liedel, *Chem. – Eur. J.*, 2017, **23**, 11810–11817.
3 S. Kirchhecker, M. Antonietti and D. Esposito, *Green Chem.*, 2014, **16**, 3705; D. Esposito, S. Kirchhecker and M. Antonietti, *Chem. – Eur. J.*, 2013, **19**, 15097.
4 T. Welton, *Chem. Rev.*, 1999, **99**, 2071; P. Wasserscheid and W. Keim, *Angew. Chem., Int. Ed.*, 2000, **39**, 3772.
5 R. P. Swatloski, S. K. Spear, J. D. Holbrey and R. D. Rogers, *J. Am. Chem. Soc.*, 2002, **124**, 4974; A. Brandt, J. Gräsvik, J. P. Hallett and T. Welton, *Green Chem.*, 2013, **15**, 550.
6 K. C. Badgujar and B. M. Bhanage, *Bioresour. Technol.*, 2015, **178**, 2.
7 S. Song, M. Kotobuki, F. Zheng, Q. Li, C. Xu, Y. Wang, W. D. Z. Li, N. Hu and L. Lu, *J. Electrochem. Soc.*, 2017, **164**, A741; K. A. Francis, C.-W. Liew, S. Ramesh and K. Ramesh, *Ionics*, 2016, **22**, 919; F. Lu, X. Gao, A. Wu, N. Sun, L. Shi and L. Zheng, *J. Phys. Chem. C*, 2017, **121**, 17756; J. F. Vélez, L. V. Álvarez, C. del Río, B. Herradón, E. Mann and E. Morales, *Electrochim. Acta*, 2017, **241**, 517.
8 H. Ohtani, S. Ishimura and M. Kumai, *Anal. Sci.*, 2008, **24**, 1335.
9 N. de Vos, C. Maton and C. V. Stevens, *ChemElectroChem*, 2014, **1**, 1258.
10 G. H. Lane, *Electrochim. Acta*, 2012, **83**, 513.
11 B. Wang, L. Qin, T. Mu, Z. Xue and G. Gao, *Chem. Rev.*, 2017, **117**, 7113.
12 Y. Chu, H. Deng and J.-P. Cheng, *J. Org. Chem.*, 2007, **72**, 7790.
13 B. Gorodetsky, T. Ramnial, N. R. Branda and J. A. C. Clyburne, *Chem. Commun.*, 2004, 1972; A. J. Arduengo, R. L. Harlow and M. Kline, *J. Am. Chem. Soc.*, 1991, **113**, 361.
14 T. Kakibe, N. Yoshimoto, M. Egashira and M. Morita, *Electrochem. Commun.*, 2010, **12**, 1630.
15 A. Bakac, V. Butkovic, J. H. Espenson, J. Lovric and M. Orhanovic, *Inorg. Chem.*, 1989, **28**, 4323.
16 V. Strehmel, A. Laschewsky, H. Wetzel and E. Görnitz, *Macromolecules*, 2006, **39**, 923.
17 E. I. Izgorodina, R. Maganti, V. Armel, P. M. Dean, J. M. Pringle, K. R. Seddon and D. R. MacFarlane, *J. Phys. Chem. B*, 2011, **115**, 14688.
18 S. Gardner, T. Kawamoto and D. P. Curran, *Org. Synth.*, 2015, **92**, 342.
19 S. Gardner, T. Kawamoto and D. P. Curran, *J. Org. Chem.*, 2015, **80**, 9794.
20 S. Huang, X. Qi, T. Liu, K. Wang, W. Zhang, J. Li and Q. Zhang, *Chem. – Eur. J.*, 2016, **22**, 10187.
21 D. P. Curran, A. Solovyev, M. Makhlouf Brahmi, L. Fensterbank, M. Malacria and E. Lacôte, *Angew. Chem., Int. Ed.*, 2011, **50**, 10294.
22 A. S. M. C. Rodrigues, C. F. R. A. C. Lima, J. A. P. Coutinho and L. M. N. B. F. Santos, *Phys. Chem. Chem. Phys.*, 2017, **19**, 5326.
23 E. Gómez, N. Calvar, Á. Domínguez and E. A. Macedo, *Ind. Eng. Chem. Res.*, 2013, **52**, 2103.
24 A. R. Choudhury, N. Winterton, A. Steiner, A. I. Cooper and K. A. Johnson, *J. Am. Chem. Soc.*, 2005, **127**, 16792.
25 B. Wrackmeyer, *Prog. Nucl. Magn. Reson. Spectrosc.*, 1979, **12**, 227.
26 E. Scholz, *Karl Fischer Titration*, Springer, Berlin, Heidelberg, 1984.
27 S. Fendt, S. Padmanabhan, H. W. Blanch and J. M. Prausnitz, *J. Chem. Eng. Data*, 2011, **56**, 31; J. Jacquemin, P. Husson, A. A. H. Padua and V. Majer, *Green Chem.*, 2006, **8**, 172.
28 S. Tang, G. A. Baker and H. Zhao, *Chem. Soc. Rev.*, 2012, **41**, 4030.
29 J. C. Crittenden, R. R. Trussell, D. W. Hand, K. J. Howe and G. Tchobanoglous, *MWH's Water Treatment*, John Wiley & Sons, Inc, Hoboken, 2012.
30 R. S. Lenk, ed., *Polymer Rheology*, Springer, Netherlands, Dordrecht, 1978.